Supporting Information

Park et al. 10.1073/pnas.1406473111

SI Materials and Methods

ATP Bioluminescence Assay. CD1d-tetramer-enriched iNKT cells were stained with antibodies specific for NK1.1 and CD44. Next, 10^4 NK1.1$^-$CD44$^-$ iNKT cells were sorted and lysed. Basal ATP levels were determined using an ATP bioluminescence assay kit HS II according to the manufacturer's protocol (Roche) with a microplate luminometer.

Bone Marrow Chimeras. Mixed bone marrow chimeras were generated using a 1:1 mixture of B6.SJL-Ptprc^{a}Pepc^b/BoyJ (CD45.1) and Folliculin-interacting protein 1 (*Fnip1*)$^{-/-}$ (CD45.2) mice. Next, 5×10^6 CD45.1 and CD45.2 bone marrow cells were transferred into lethally irradiated (900 rad) $Rag2^{-/-}\gamma_c^{-/-}$ mice. Bone marrow chimeras were analyzed 10 wk after transfer.

Quantitative Real-Time PCR. To purify stage 1, stage 2, and stage 3 invariant natural killer T (iNKT) cells, CD1d tetramer-enriched thymocytes were sorted based on CD44 and NK1.1 profiles using a FACSAria flow cytometer. RNA was extracted using RNAqueous-Micro kit (Ambion). cDNA was made using SuperScript II reverse transcriptase (Invitrogen). cDNA was subjected to real-time PCR using *Fnip1*, *Gapdh*, and *PLZF*-specific primers. Primer sequences were as follows: *Fnip1* forward 5′-TGGAAGATCTTTGCTGGGTGGCTA-3′ and reverse 5′-GCTGGCCACTTGAACAGTCCATTT-3′; *Gapdh* forward 5′-TGCACCACCAACTGCTTAG-3′ and reverse 5′-GAGGCAGGGATGATGTTC-3′; *PLZF* forward 5′-GAGCAGTGCAGCGTGTGT-3′ and reverse 5′-AACCGTTTTCCGCAGAGTT-3′; *Vα14* forward 5′-TGGGAGATACTCAGCAACTCTGG-3′; *Jα18* reverse 5′-CAGGTATGACAATCAGCTGAGTCC-3′; quantitative PCR analysis of transcripts of Vα14 and Vα3 rearrangements to Jα56, Jα18, and Jα9 was described previously (1–3). Results were normalized to Cα transcript using the following primers: Cα forward 5′- CCTCTGCCTGTTCACCGACTT-3′ and Cα reverse 5′-TGGCGTTGGTCTCTTTGAAG-3′. PCR amplification was performed with the Brilliant qPCR kit (Stratagene) using an Applied Biosystems 7300 Real-Time PCR System.

Flow Cytometry and Cell Sorting. Thymus, spleen, and liver cells were stained with fluorescent-conjugated antibodies specific for NK1.1, T-cell receptor-β (TCR-β), TCR-γδ, CD4, CD8, B220, IgM, CD45.1, CD45.2, CD24, CD44, CD244.2, CD94, CD69, CD122, Ly-49G2, CD1d, CD150, CD1d/αGalCer dimer (BD DimerX), mCD1d/PBS57 (National Institutes of Health tetramer core facility, Emory University, Atlanta, GA), and NKG2D. Intracellular staining for phospho-S6 ribosomal protein (Ser-235/236; Cell signaling), Rorγt, early growth response protein 2 (Egr2), Runt-related transcription factor (Runx)1, T-box transcription factor, Tbx21 (T-bet), and promyelocytic leukaemia zinc finger (PLZF) were performed according to the manufacturer's protocol (eBioscience). CD1d/αGalCer dimer and mCD1d/PBS57 tetramer are designated as "CD1d tetramer" for convenience in the text.

In Vivo BrdU Labeling and Apoptosis Assays. Mice were given 0.8 mg/mL BrdU (Sigma-Aldrich) by intraperitoneal injection. Total thymocytes were harvested 24 h later, stained with biotinylated CD1d dimer, and enriched by the MACS system. Purified cells or total thymocyte were surface-stained with antibodies specific for CD44 and NK1.1 or with CD1d tetramer and TCR-β. Cells were fixed, permeabilized, and treated with 30 μg DNase I (Sigma-Aldrich). Incorporation of BrdU into DNA was measured by flow cytometry using anti–BrdU-FITC (BD Biosciences) according to the manufacturer's protocol. Apoptosis was detected with CellEvent Caspase 3/7 green detection (Life Technologies) system and dead cells were excluded with near-IR dead cell stain kit (Life Technologies).

Analysis of Mitochondrial Mass and Superoxide Production. Thymocytes from WT and *Fnip1*$^{-/-}$ mice were stained with MitoTracker Green FM (25 nM) or MitoSox (5 μM; Life Technologies) in conjunction with CD1d tetramer, CD44, NK1.1. Cells in culture media [RPMI/5% (vol/vol) FBS] were incubated for 30 min at 37 °C.

1. D'Cruz LM, Knell J, Fujimoto JK, Goldrath AW (2010) An essential role for the transcription factor HEB in thymocyte survival, Tcra rearrangement and the development of natural killer T cells. *Nat Immunol* 11(3):240–249.
2. Hu T, Simmons A, Yuan J, Bender TP, Alberola-Ila J (2010) The transcription factor c-Myb primes CD4+CD8+ immature thymocytes for selection into the iNKT lineage. *Nat Immunol* 11(5):435–441.
3. Gapin L, Matsuda JL, Surh CD, Kronenberg M (2001) NKT cells derive from double-positive thymocytes that are positively selected by CD1d. *Nat Immunol* 2(10):971–978.

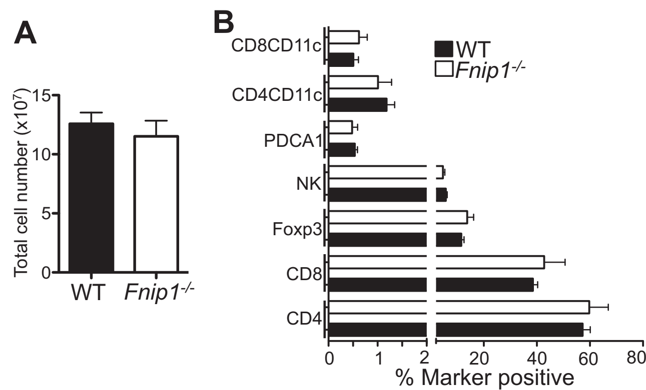

Fig. S1. Normal total number of thymocytes and representation of splenic CD4, CD8, T regulatory (Treg), NK, and dendritic cells in *Fnip1*$^{-/-}$ mice. (*A*) Total thymocyte numbers are shown (*n* = 5 mice per group). (*B*) Splenocytes were stained for CD4 (*n* = 9 mice per group), CD8 (*n* = 6 mice per group), Foxp3 (*n* = 4 mice per group), PDCA1 (*n* = 6 mice per group), CD11c (*n* = 5 mice per group), TCR-β, B220, and NK1.1 (*n* = 8 mice per group). Cells that fall within the specified gates are displayed by the mean percentage (relative to TCR-β^{+} or B220^{-} cells) ± SEM.

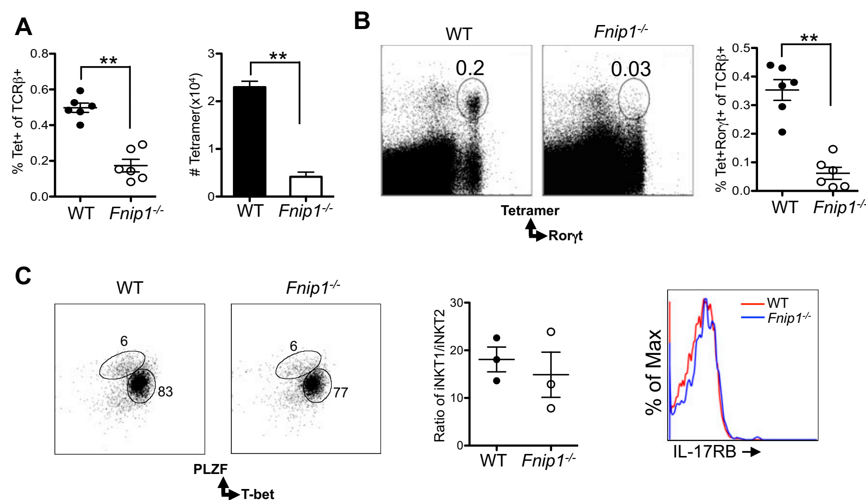

Fig. S2. Analysis of different lineages of iNKT cells in *Fnip1*$^{-/-}$ mice. (*A* and *B*) Cells from inguinal and axillary lymph nodes were stained with TCR-β, CD1d tetramer, and intracellular Rorγt. (*A*) The percentage and total number of Tet^{+}TCR-β^{+} cells are reduced in *Fnip1*$^{-/-}$ mice. (*B*) A separate lineage of *Rorγt*$^{+}$ iNKT cell (iNKT17) development is greatly impaired in *Fnip1*$^{-/-}$ mice. (*C*) Ratio of iNKT1:iNKT2 cells is not altered in splenic *Fnip1*$^{-/-}$ iNKT cells. Splenocytes from WT and *Fnip1*$^{-/-}$ mice were stained with CD1d tetramer, anti–TCR-β, and intracellular PLZF and T-bet. The ratios of PLZF^{high}T-bet^{low} (iNKT2) and PLZF^{low}T-bet^{high} (iNKT1) within tetramer-positive cells are shown. For IL-17RB staining, cells were stained with CD1d tetramer and antibodies specific to CD4 (IgG2b) and IL-17RB (MBL, B5F6) followed by staining with anti IgG2a FITC. Histogram for IL-17RB is shown within CD4^{+}CD1d^{+} cells. Representative FACS dot-plots and histogram are shown from three to six mice per group. Shown are the mean ± SEM. $^{**}P < 0.0001$ (unpaired *t* test).

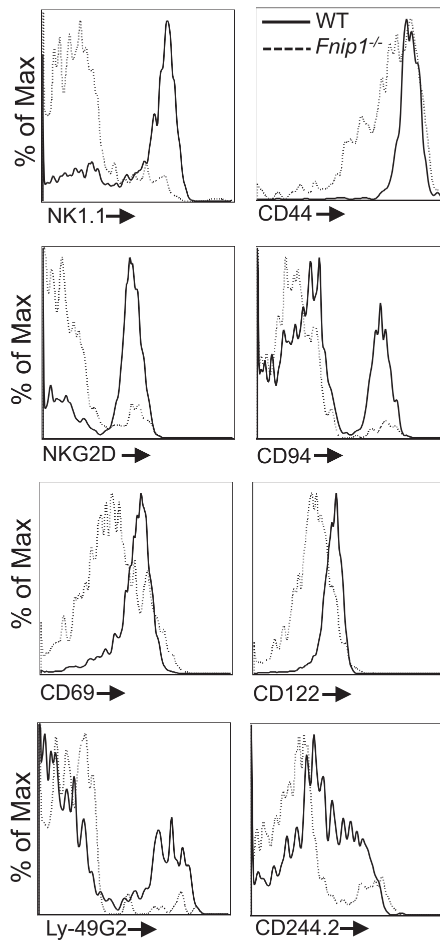

Fig. S3. iNKT cells from *Fnip1*$^{-/-}$ mice are arrested at an immature cell stage. Thymic CD1d tetramer-positive cells were stained with antibodies specific for the indicated surface proteins. Shown are representative flow cytometric histogram from n = 3 mice per group.

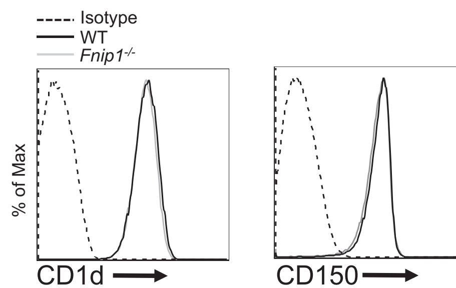

Fig. S4. CD1d and CD150 (SLAM, signaling lymphocyte activation molecule) are expressed normally on *Fnip1*$^{-/-}$ thymocytes. Thymocytes were stained with antibodies specific for CD4, CD8, CD1d, and CD150. Expression of CD1d and CD150 were analyzed on CD4^{+}CD8^{+} double-positive (DP) thymocytes. Representative FACS histograms are shown from n = 3 mice per group.

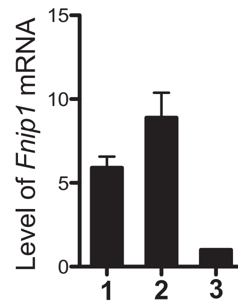

Fig. S5. *Fnip1* expression is decreased in Stage 3 iNKT cells relative to stage 1 and 2 iNKT cells. Total iNKT cells were enriched from WT thymocytes by tetramer selection using magnetic beads. iNKT developmental subsets were FACS-sorted based on CD44 and NK1.1 expression and *Fnip1* and *Gapdh* expression were analyzed by real-time PCR. Shown is the mean ± SEM of three mice per group.

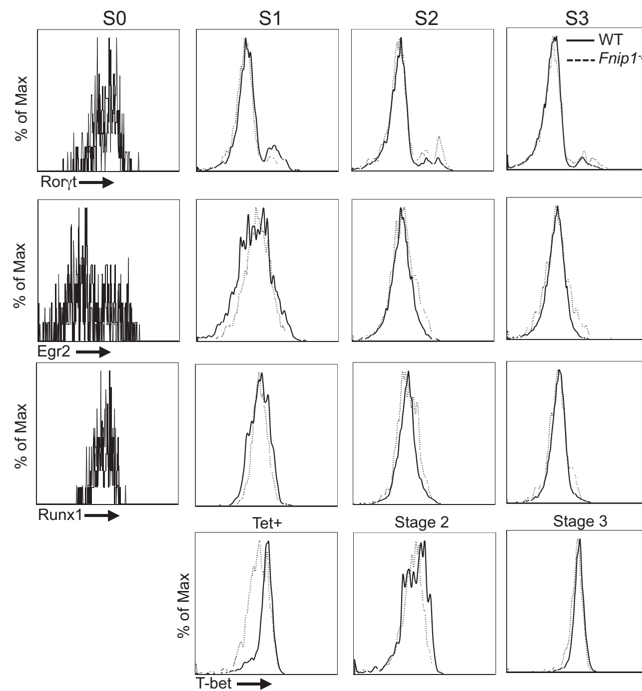

Fig. S6. Intracellular staining for Rorγt, Egr2, Runx1, and T-bet proteins during development of *Fnip1*$^{-/-}$ and WT iNKT cells. Cells were stained with CD24, CD44, NK1.1, CD1d tetramer, and intracellular Rorγt, Egr2, and Runx1. Intracellular staining for T-bet was performed on thymocytes stained with NK1.1, CD44, and CD1d tertramer. Data are representative of five mice (stage 0 of Rorγt, Egr2, Runx1), and seven mice (T-bet) per group.

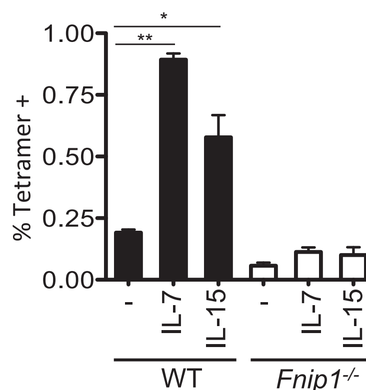

Fig. S7. Reduced *Fnip1*$^{-/-}$ iNKT precursor cell response following culture in IL-7 and IL-15. Total thymocytes (5×10^6 cells) were cultured in 24-well plates for 48 h in the presence of cytokines (each 10 ng/mL). Cells were stained with TCR-β and CD1d tetramer. Shown is the mean ± SEM of $n = 3$ mice per group. *$P < 0.05$ (unpaired *t* test), **$P < 0.0001$ (unpaired *t* test).

Fig. S8. Transgenic expression of IL-7Rα or deficiency of Bim1 fails to restore iNKT cell maturation in *Fnip1*$^{-/-}$ mice. Thymocytes were stained with NK1.1, TCR-β, and CD1d tetramer. Shown are data representative from three mice (IL-7Rα Tg) and four mice (*Bim1*$^{-/-}$) per group.

Fig. S9. *Fnip1*$^{-/-}$ iNKT cells have increased reactive oxygen species. Thymic iNKT cells were analyzed with CD44, NK1.1, CD1d tetramer, and MitoSox (5 μM). Cells in culture media (RPMI/5% FBS) were incubated for 30 min at 37 °C for MitoSox according to the manufacturer's protocol (Life Technologies). The mean ± SEM of the percentage of MitoSox-positive iNKT cells (*Left*) and stage 1, 2, and 3 iNKT cells (*Right*) is shown from five mice per group. *$P < 0.05$ (unpaired *t* test).